



Missouri University of Science and Technology
Scholars' Mine

Symposia on Turbulence in Liquids

Chemical and Biochemical Engineering

06 Oct 1971

Wavevector/Frequency Spectrum of Turbulent-Boundary-Layer Pressure

D. M. Chase

Follow this and additional works at: <https://scholarsmine.mst.edu/sotil>

 Part of the [Chemical Engineering Commons](#)

Recommended Citation

Chase, D. M., "Wavevector/Frequency Spectrum of Turbulent-Boundary-Layer Pressure" (1971). *Symposia on Turbulence in Liquids*. 80.

<https://scholarsmine.mst.edu/sotil/80>

This Article - Conference proceedings is brought to you for free and open access by Scholars' Mine. It has been accepted for inclusion in Symposia on Turbulence in Liquids by an authorized administrator of Scholars' Mine. This work is protected by U. S. Copyright Law. Unauthorized use including reproduction for redistribution requires the permission of the copyright holder. For more information, please contact scholarsmine@mst.edu.

WAVEVECTOR/FREQUENCY SPECTRUM OF TURBULENT-BOUNDARY-LAYER PRESSURE

David M. Chase
 Bolt Beranek and Newman, Inc.
 Cambridge, Massachusetts 02138

ABSTRACT

Knowledge of the wavevector/frequency spectrum of wall pressure, $P(\bar{K}, \omega)$ [$\bar{K} = (k_1, k_3)$], for a normal turbulent boundary layer has been largely confined to properties depending on the mean-convective ridge ($k_1 = \omega/u_c$). Recent theoretical work yields the wavevector dependence of $P(\bar{K}, \omega)$, for flow at low Mach numbers, also in the acoustic wave number domain where $K \leq \omega/c$, except for undetermined functions of $\omega \delta / U_\infty$. In the nonconvective but incompressible domain of wavevectors (important in underwater acoustics), apart from the proportionality to K^2 where $\omega/c \leq K \leq \delta^{-1}$, the scaling, dependence and magnitude of $P(\bar{K}, \omega)$ remain to be established.

This domain is approached here by theoretical modeling of the velocity-derivative sources of pressure. The expression for the pressure spectrum derived from the pertinent Poisson equation is cast so that source models may be formulated as spectra in frequency and three-component wavevector, and inhomogeneity normal to the wall treated via dependence of source strength, correlation scales, and mean convection velocity on geometric mean wall distance. A model for the frequency dependence is formulated on the notion of fluctuating local convection. Convection of a frozen wave pattern of the turbulent velocity-product field generates a disturbance in this velocity product, and hence in wall pressure, at frequency ω even if the streamwise wavenumber component of the convected pattern is much smaller than the minimum mean convective wavenumber, ω/U_∞ . Such generation occurs by virtue of wavenumber components normal to the wall on the order of the ratio of frequency to probable normal convection velocities. The effective rms normal convection velocity is argued to be of the order of the local rms normal turbulence velocity. (This local-convection model for pressure differs essentially from one based jointly on assumption of a space-time quasinormal velocity distribution and application of the local-convection model to two-component velocity spectra.) The model yields the source wavevector/frequency spectrum in terms of the pure wavevector spectrum. A wavevector spectrum constructed to accord with Kronauer-Morrison wave structure yields, in the nonconvective domain where $(\omega - u_c k_1) / v_* K \gg 1$ (v_* = friction velocity) but $K \delta \gg 1$:

$$P(\bar{K}, \omega) = a' B(k_1/K) \rho^2 v_*^7 K (\omega - u_c k_1)^{-4} \quad (A)$$

for $\Omega \ll 1$, where a' is a constant, $B(k_1/K)$ an uncertain anisotropy factor, u_c a convection velocity, and $\Omega = 5(\omega - u_c k_1) \nu / v_*$ a viscous-sublayer parameter; for $\Omega \gg 1$, an exponential cutoff is predicted. This sharp cutoff is characteristic of the local-convection model with a normal distribution of convection velocity. An alternative source wavevector spectrum yields form (A) with an additional factor $v_* K (\omega - u_c k_1)^{-1}$. A recent wind-tunnel measurement is interpreted to provide an upper limit on a' in either case.

Application of the model to the mean-convective domain suggests isotropy of the pertinent Kronauer-Morrison wave strength and hence an angular dependence of $P(K, \omega)$ as

$c_t + c_m (k_1/K)^2$, where c_t, c_m derive respectively from pure-turbulence and mean-shear source terms and c_t/c_m is comparable with or somewhat less than unity.

INTRODUCTION

We discuss a model for deriving the wall pressure beneath a turbulent boundary layer (TBL) with regard to its spectral density in wavevector and frequency - particularly at low, nonconvective wavenumbers - and also briefly review a recent calculation at still lower, acoustic wavenumbers. Explicit attention is confined to an equilibrium boundary layer on a smooth, stationary, rigid plane in flow at low Mach number without mean pressure gradient. Streamwise inhomogeneity associated with boundary-layer growth is neglected, so that a unique spectral density of pressure in two wavevector components and frequency is indeed definable.

In Fig. 1 is roughly represented the wavevector spectrum of TBL wall pressure at given frequency. The lower part constitutes the trace in the plane $k_3 = 0$, k_1 being streamwise. The spectrum is substantially characterized by four reciprocal length scales indicated along the abscissa: (1) acoustic wavenumber ω/c , (2) reciprocal outer eddy scale, proportional

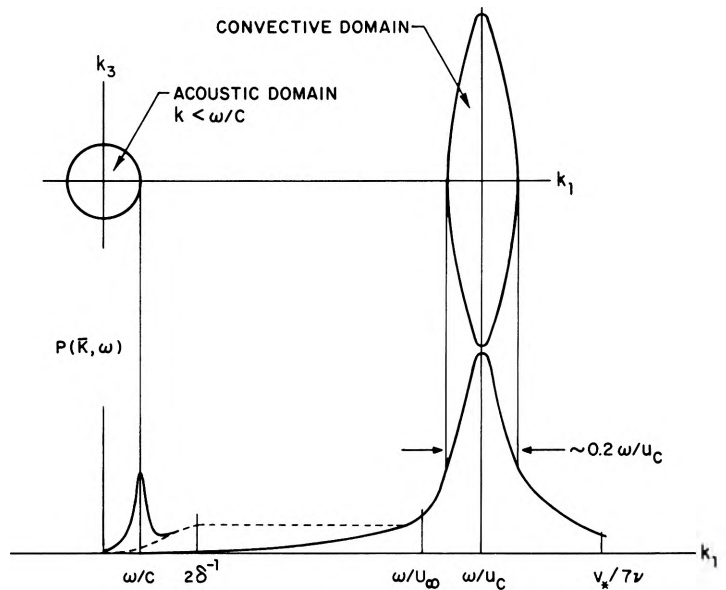


Fig. 1 Wavevector Spectrum of Turbulent-Boundary-Layer Pressure

to δ^{-1} , where δ denotes boundary-layer thickness, (3) minimum mean-convective wavenumber, ω/U_∞ , (4) reciprocal viscous-sublayer thickness, $v_*/7\nu$, where v_* is the wall-friction velocity. Except as noted, the ordering of these scales will be assumed as shown in the figure. Also indicated is a wavenumber, ω/u_c , where u_c denotes a mean phase velocity defined by longitudinal cross-spectral density. This wavenumber lies near the summit of the mean-convective ridge of $P(\bar{K}, \omega)$. A hypothetical contour of the convective ridge in the k_1 - k_3 plane is displayed in the upper part of the slide.

Above the acoustic region ($K \sim \omega/c$), the dependence of $P(K, \omega)$ is known to be as K^2 , but above the next characteristic wavenumber scale, $\sim 2\delta^{-1}$, the dependence is presently uncertain. Two possibilities are depicted: (1) the K^2 dependence persists; (2) the spectrum levels off to become wavenumber-white up to the mean-convective domain where $k_1 > \omega/U_\infty$.

If the TBL pressure were generated purely by "frozen" eddies convected downstream at mean velocities not exceeding the free-stream velocity, or by fluctuating-velocity waves with analogous phase velocities, the spectral density would vanish for all $k_1 < \omega/U_\infty$.

Choice of the wavevector-frequency spectral density for the two-point statistical description of the wall-pressure field is preferred on account of its domains of distinctive behavior characterized by subsets of the wavenumber scales. In typical applications, moreover, quantities of interest may be expressed as the wavevector integral of a simple product of the driving spectrum $P(\bar{K}, \omega)$ by a response function.

In underwater applications to flow-induced self-noise and radiation, there is a great disparity between the low wavenumbers where system response is relatively high because of area averaging or peaked because of resonance of the flow-bounding wall, and the high wavenumbers where the TBL pressure has its convective ridge. Hence the magnitude and dependence of spectral density of pressure at low, "non-convective" wavenumbers has special importance.

Nevertheless, the bulk of experimental and theoretical work on TBL pressure through the years has dealt with properties dominated by the convective ridge. This implicit emphasis in laboratory work is due in part to the difficulty of keeping spurious acoustic noise at a sufficiently low level while suppressing high-wavenumber TBL noise by a suitable system response, in part to difficulty in sensitively controlling boundary conditions on a pressure transducer to achieve this high-wavenumber suppression, and in part, no doubt, to historical accident.

A good deal is known, then about properties of the spectral density related to the convective ridge in the instance of a normal TBL, and in recent years most experimental investigation has been directed rather to modified TBL's, for example, those with rough walls, mean pressure gradients, or polymer injection. Among properties of the convective domain established in a substantial region of parameter space are the wavevector-integrated point pressure spectrum, similarity characteristics, phase convection velocity, and principal widths of the convective ridge. Even for a normal boundary layer, however, significant properties remain undetermined. For example, the shape of contours of the ridge in \bar{K} -space at fixed ω remains uncertain beyond the fact that their extension in the k_3 direction is about seven times that in k_1 (this ratio being inverse to that of narrow-band correlation distances in spanwise and streamwise directions).

DISCUSSION

1. The Acoustic Domain

In the acoustic domain where $K \leq \omega/c$, the wavenumber dependence of $P(\bar{K}, \omega)$ was treated by Bergeron¹ by the method of matched

asymptotic expansions² applied to the singular perturbation problem represented by the differential equation for the Fourier amplitude of pressure as a function of wall distance. For a strictly incompressible boundary layer, the pressure spectrum varies as K^2 as $K\delta \rightarrow 0$, but for one with nonvanishing compressibility, however small, it remains finite there³. Bergeron obtained the rather remarkable further result that the (Lighthill) pressure-source functions, to lowest order, remain unaltered by compressibility even at the acoustic wavenumber, $K = \omega/c$, and that the pressure spectral density, under the idealized assumptions, consequently has a nonintegrable singularity there. He obtained explicitly the \bar{K} -dependence of $P(\bar{K}, \omega)$ in the acoustic domain but with 24 undetermined functions of $\omega\delta/v_*$ still involved. In the neighborhood of the singularity, in particular, $P(\bar{K}, \omega)$ may be written as:

$$P(\bar{K}, \omega) = (v_*/c)^2 \rho^2 v_*^6 \omega^{-3} [1 - (cK/\omega)^2]^{-1} F(\omega\delta/v_*, \cos\theta) \quad (1)$$

with $\cos\theta = k_1/K$, in which the function F can be written with its dependence on the direction variable θ made explicit in terms of eight unknown functions of $\omega\delta/v_*$.

This nonphysical result - an infinite point pressure spectrum - reflects the assumed infinite extent of the boundary layer. For a boundary layer of finite linear dimensions $-L$, Bergeron found Equation 1 to be valid for K outside a fractional interval on the order of $(\omega L/c)^{-1}$ near the acoustic wavenumber ω/c and estimated the contribution of the acoustic domain to the wavevector-integrated pressure spectrum as given by:

$$\int_{k_1 = \omega/c}^{\infty} d\bar{K} P(\bar{K}, \omega) \sim (v_*/c)^4 \rho^2 v_*^4 \omega^{-1} f(\omega\delta/v_*) \ln(\omega L/c). \quad (2)$$

For a likely order of magnitude of the undetermined function f in Equation 2, this TBL contribution from the acoustic domain is typically small by virtue of the smallness of v_*/c .

2. Further Use of Matched Asymptotic Expansions

The method of matched asymptotic expansions may have utility also in the incompressible but nonconvective wavenumber domain where $K\delta \geq 1$ but $Kv_*/\omega \ll 1$. In the prior application to the domain $K\delta \ll 1$ for compressible (and incompressible) flow, Bergeron could derive the wavevector dependence of $P(\bar{K}, \omega)$ explicitly, because in the outer region the source functions vanished and the form of the solution for pressure there was known. In application to domains where the outer region lies within the boundary layer, on the other hand, we can aspire at most to obtain useful simple relations between limiting properties of source functions and the resulting dependence of pressure.

Formal application of the method to the differential equation for pressure in both the Landahl form⁴ (essential to success in Bergeron's problem) and the Poisson form⁵ suggests possible relations between limiting forms of four-component and two-component velocity correlations.

The method can be pursued also into the viscous sublayer, involving new inner and outer scales, with the objective to investigate the basis for the approximation (assumed by Bergeron and in our work to follow) that the normal derivative of pressure at given \bar{K}, ω vanishes at the wall.

3. Approximate Formulation of the Wall-Pressure Spectrum in Terms of Velocity-Derivative Spectra

The work presented hereafter consists in explicit descrip-

tive modeling of the TBL pressure sources, grounded on crude notions of kinematics and current views of boundary-layer wave structure and similarity.[#] Deeper dynamic analysis is not attempted.

Formulation of the model involves three main parts: first, approximate relation of the pressure spectrum to a source spectrum of character convenient for source modeling; second, introduction of a local-convection model for the time dependence of the source spectrum in a mean convected frame; and, third, modeling of the source spectrum at fixed time on the basis of experimental properties of fluctuating velocity and pressure spectra.

To lay the groundwork, we formulate a convenient approximate relation of the pressure spectrum to velocity spectra, proceeding in standard fashion from the Poisson equation for pressure in incompressible flow in terms of the velocity-derivative sources:

$$\nabla^2 p = -\rho [\partial_1 \partial_j v_1 v_j + 2 u'(x_2) \partial_1 v_2] \quad (3)$$

These sources are separated in Eq. 3 into a set of "pure-turbulence" terms involving products of fluctuating components, v_i , and a "mean-shear" term involving the product of mean-flow gradient, $u'(x_2)$, and the normal fluctuating component, a sum over repeated indices being understood. This equation is Fourier-transformed over time and over spatial coordinates in the plane of the wall, formally solved in the usual way, and those pure-turbulence terms involving derivatives normal to the wall are integrated by parts. A product of Fourier amplitudes of pressure at the wall is then statistically averaged to yield the wavevector-frequency spectrum $P(\bar{k}, \omega)$. This is composed of a pure turbulence term, P_t , a mean-shear term, P_m , a cross term, and in addition a term proportional to the squared normal derivative of pressure at the wall and associated cross terms. We neglect the pressure derivative, as usual, and consider only P_t and P_m , proceeding explicitly only with P_t . P_t is related to a source function $\bar{\sigma}$ by the equation:

$$P_t(\bar{k}, \omega) = \rho^2 k^2 \int_0^\infty dx_2 \int_0^\infty dx_2' \exp[-K(x_2 + x_2')] \bar{\sigma}(x_2, x_2', \bar{k}, \omega) \quad (4)$$

$\bar{\sigma}$ is the spectral density in \bar{k} and ω of a linear combination of two-component velocity products, $v_1(\bar{x}, t)v_j(\bar{x}, t)$, the correlated products referring respectively to wall distances x_2, x_2' , as expressed by the following equations:

$$\bar{\sigma}(x_2, x_2', \bar{k}, \omega) = \langle \hat{S}^*(x_2, \bar{k}, \omega) \hat{S}(x_2', \bar{k}', \omega') \rangle / \delta(\bar{k}' - \bar{k}) \delta(\omega' - \omega) \quad (5)$$

$$\hat{S} = -(\theta_1^2 \hat{T}_{11} + 2\theta_1 \theta_3 \hat{T}_{13} + \theta_3^2 \hat{T}_{33}) + 12(\theta_1 \hat{T}_{12} + \theta_3 \hat{T}_{32}) + \hat{T}_{22} \quad (6)$$

$$\hat{T}_{ij}(x_2, \bar{k}, \omega) = (2\pi)^{-3} \int d^2 \bar{x} \int dt \exp[-i(\bar{k} \cdot \bar{x} - \omega t)] v_i(\bar{x}, t) v_j(\bar{x}, t) \quad (7)$$

$$\text{where } \bar{x} = (x_1, x_2, x_3) \quad \bar{k} = (k_1, k_3) \quad \theta_i = k_i/K \quad (8)$$

(Angular brackets here denote a statistical average and integrals run over the range $-\infty$ to ∞ in each variable unless noted.)

The source spectrum $\bar{\sigma}$ may be expected to vary with its wall distance arguments x_2 and x_2' somewhat as the product of the turbulence intensities at these distances. In any case, it

facilitates model prescription to imagine an intensity profile $A(x_2, x_2')$ to be factored out of $\bar{\sigma}$ and to express the remaining normalized source spectrum as a transform over normal wavevector component of a spectral density, M , as given by:

$$\bar{\sigma}(x_2, x_2', \bar{k}, \omega) = A(x_2, x_2') \int_{-\infty}^{\infty} dk_2 \exp(ik_2 \zeta_2) M(\xi, \bar{k}, \omega) \quad (9)$$

where $\bar{k} = (k_1, k_2, k_3)$. M is thus the spectral density in frequency and in full three-dimensional wavevector of a linear combination of normalized velocity products. It retains a residual dependence on x_2 and x_2' via a single variable which we choose to be the geometric mean wall distance, ξ . The independent variables replacing x_2 and x_2' are thus ξ and the normal separation ζ_2 as given by:

$$\zeta_2 = x_2' - x_2, \quad \xi = (x_2 x_2')^{1/2} \quad (10)$$

So far, there is no approximation, since, for the actual $\bar{\sigma}$ and any choice of A, M can be defined to satisfy Eq. 9. By this maneuver, however, we may introduce plausible models for M by regarding M as depending on ξ only via the spatial scales of the related velocity correlations (and perhaps via a mean convection velocity).

We take the source profile A to have the form given by:

$$A(x_2, x_2') = w(\xi) \sum_j c_j \exp[-(x_2 + x_2')/\delta_j] \quad (11)$$

where the c_j are numerical constants and the δ_j constant length scales. The sum of exponentials is specified to approximate the variation of the source profile well outside the sublayer and the factor $w(\xi)$ to approximate the variation within and just outside the sublayer. Hereafter we retain only a single exponential term scaled by boundary-layer thickness, but recognize a probable contribution scaled by ν/v_* and associated with source points not far outside the sublayer [Ref. 7, Fig. 26]:

$$\delta_1 \propto \delta, \quad \delta_2 \propto \nu/v_* \quad (12)$$

With the model forms to be ascribed to the source spectrum M , the assumed profile (Eq. 11) cannot be expected to hold when x_2 and x_2' are not both within or outside the sublayer, but this limitation is not serious. Use of Eq. 9 and Eq. 11 in the earlier equation for the pressure spectrum yields, by integration over the normal separation ζ_2 , the result:

$$P_t(\bar{k}, \omega) = 4\rho^2 k^2 \int_0^\infty d\xi \xi w(\xi) \int_{-\infty}^{\infty} dk_2 M(\xi, \bar{k}, \omega) \times \sum_j c_j K_0(2\xi [k_2^2 + (K + \delta_j^{-1})^2]^{1/2}) \quad (13)$$

where K_0 denotes the usual modified Bessel function. For a plausible spectrum, M , the dependence of the pressure spectrum as K^2 persists at least for K smaller than the reciprocal scale of the intensity profile.

With omission of Reynolds-number dependence, the pressure spectral density must have the functional form:

$$P(\bar{k}, \omega) = \rho^2 v_*^6 \omega^{-3} F(\bar{k}v_*/\omega, \omega\delta/v_*, \omega\nu/v_*^2) \quad (14)$$

and, with the source profile A defined as dimensionless, M must have the form:

$$M(\xi, \bar{k}, \omega) = v_*^3 \xi^4 \psi(\bar{k}\xi/v_*, \omega\xi/v_*, \xi/\delta, v_*\xi/\nu) \quad (15)$$

[#] Part of this work was previously reported in Reference 6.

According to a trivial model where source velocity is time-independent in a frame traveling downstream at mean convection velocity, u_c , M would be given in terms of a pure wavevector spectrum by:

$$M(\xi, \bar{k}, \omega) = M(\xi, \bar{k}) \delta(\omega - u_c k_1) \quad u_c = u_c(\xi, \bar{k}) \quad (16)$$

To treat the non-convective tail where $k_1 < \omega/U_\infty$, however, we require a more refined description. This brings us to the core of the present approach.

4. Basis and Formulation of a Local-Convection Model for Pressure

The model proposed for the generation of pressure in the non-convective domain is based on the notion of fluctuating local convection. According to this concept, a conditional space-time correlation function is defined in a frame moving with a local convection velocity, \bar{w} say, that is itself a random variable with probability density $P(\bar{w})$, but this velocity is determined by larger-scale motion from which the local decorrelating motion is considered statistically independent. Neglect of time dependence of the correlation in the local co-moving frame then constitutes the local-convection approximation and yields the space-time correlation in the laboratory frame, $\psi(\bar{r}, \tau)$, say, in terms of the spatial correlation at zero time delay, $\psi(\bar{r}, 0)$, as in Eq. 17, or the wavevector frequency spectrum, $E(\bar{k}, \omega)$, in terms of the ordinary wavevector spectrum, $E(\bar{k})$, as in Eq. 18:

$$\psi(\bar{r}, \tau) = \int d^3 \bar{w} P(\bar{w}) \psi(\bar{r} - \bar{w}\tau, 0) \quad (17)$$

$$E(\bar{k}, \omega) = E(\bar{k}) \int d^3 \bar{w} P(\bar{w}) \delta(\omega - \bar{w} \cdot \bar{k}) \quad (18)$$

$$\text{where } E(\bar{k}) = \int d\omega E(\bar{k}, \omega) \quad (19)$$

In the universal domain of homogeneous turbulence, this approximation has a clear, though nonrigorous, basis in Kolmogorov's principles and has been employed previously (e.g., see Refs. 8-10). In the instance of a boundary layer, on the other hand, separation of local convection from development, rotation, distortion, and decay of eddies or wave structures presently lacks any heuristic basis. Nevertheless, some qualitative effect of the nature of local convection is surely operative, and we expect the true wavevector-frequency spectra outside the domain accessible to mean convection to be at least of the order of that obtained by a suitably constructed local-convection model. Provided the pressure spectral density yielded by the model proves not to be exponentially small at low wavenumbers, the model may be conjectured to yield not only a lower limit but even a valid estimate.

A local-convection model is formulated for the source spectrum $M(\xi, \bar{k}, \omega)$ directly by reference to the prototype Eq. 18 and given by:

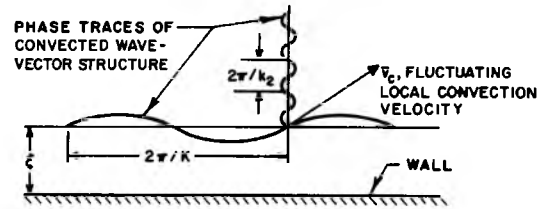
$$M(\xi, \bar{k}, \omega) = M(\xi, \bar{k}) \int d^3 \bar{v}_c P(\xi, \bar{k}, \bar{v}_c) \delta(\omega - u_c k_1 - \bar{v}_c \cdot \bar{k}) \quad (20)$$

where $u_c = u_c(\xi, \bar{k}, \omega)$, \bar{v}_c represents a fluctuating convection velocity in a mean rest frame traveling downstream at an effective convective velocity $u_c (< U_\infty)$, and P the corresponding probability density. Both P and u_c at this stage may depend on ξ and \bar{k} .

This model in fact yields a credible magnitude for the pressure spectrum in accord with the following kinematic

description (see Fig. 2). A velocity-product disturbance at frequency ω can be generated by fluctuating convection of a frozen wave pattern of the velocity-product field even if this pattern has a projected streamwise wavenumber component that is $\ll \omega/U_\infty$. For this it is required only that the wavenumber component normal to the wall be as large as the frequency divided by a normal convection velocity presumed of the order of the rms normal component of turbulent velocity. By the relation

SCHEMATIC ILLUSTRATION OF LOCAL CONVECTION MODEL



1. Convection of static wavevector pattern generates frequency $\omega = \bar{v}_c \cdot \bar{k}$ ($\approx v_{c2} k_2$ if $v_2 K \ll \omega$)
2. \bar{v}_c is regarded as spatially varying only via wavevector components $\leq |k_1|$

Fig. 2 Schematic Illustration of Local Convection Model

between pressure and derivatives of velocity products, a similarly low-wavenumber component of pressure is generated.

5. Interpretations and Alternatives in the Local-Convection Formulation

With acceptance for the moment of the local-convection equation for the frequency dependence of M , it is essential to establish whether the probability of a given local convection velocity is simply on the order of the probability of an equal fluctuating turbulent velocity at the same wall distance ξ . It might be suggested that the only contribution to $M(\xi, \bar{k}, \omega)$ sensibly estimated by a local-convection approximation is that associated with local convection velocities that are relatively uniform over a distance $\sim k_1^{-1}$ in each coordinate direction i - that is, an eddy may be viewed as convected without distortion only by larger eddies, not smaller ones - and hence that $P(\xi, \bar{k}, \bar{v}_c)$ should include only the probability density for that part of fluctuating velocity associated with wavenumber components $\leq k_1$. In the non-convective domain where $K \ll \omega/U_\infty$, the local-convective contribution, in such case, would be negligible. This result depends on the fact that, assuming the correlation scale for the normal component of fluctuating convection velocity to be on the order of wall distance, the part of this velocity component associated with low wavenumbers, K , in the plane parallel to the wall becomes suppressed at wall distance, ξ , small relative to their reciprocal, K^{-1} . An estimate based on assumption of a normal probability distribution of local convection velocity, in particular, yields a local-convection contribution to the pressure spectrum that is exponentially small in $-(\omega/v_{c2} K)^{2/3}$ at non-convective wavevectors ($k_1 < \omega/U_\infty$).

It is argued, however, that the probability density should not be restricted to include only local convection velocities at low planar wavenumbers. M , we recall, is formed from Fourier amplitudes, \hat{T}_{ij} , that are convolutions of velocity transforms as given by:

$$\hat{T}_{ij}(x_2, \bar{k}, \omega) = \int d^2 \bar{k}' \int d\omega' \hat{v}_i(x_2, \bar{k}', \omega') \hat{v}_j(x_2, \bar{k} - \bar{k}', \omega - \omega') \quad (21)$$

Now, for K small relative to the reciprocal velocity correlation scale at x_2 , most of the integral in Eq. 21 will derive from $K' \sim (\text{correlation scale})^{-1}$, even if this greatly exceeds K . Hence we should include in the pertinent convection velocity planar wavenumbers up to roughly K' , not just up to K , and the rms normal component of convection velocity is therefore of the same order as that of turbulence velocity. The spatial variation of convection velocity does modulate the convected wave structures and hence influences the wavevector composition of \hat{T}_{ij} in the spatial "beating" process (Eq. 21); still, the modulating wavenumber apparently may exceed the difference wavenumber, \bar{k} , without violating the kinematic credibility of convection.

According to a somewhat different view, a local convection velocity may be associated with a dynamically distinct, quasi-periodic primary motion that convects a superimposed random motion.

In any case, we assume the probability distribution of convection velocity to be independent of \bar{k} and given by a normal distribution characterized by the mean turbulence velocity products at wall distance ξ . This leads to the explicit frequency dependence of the source spectrum given by:

$$M(\xi, \bar{k}, \omega) = M(\xi, \bar{k}) (2\pi)^{-1/2} \omega_k^{-1} \exp[-(1/2)(\omega - u_c k_1)^2 / \omega_k^2] \quad (22)$$

where $\omega_k^2 \equiv \langle v_1^2 \rangle k_1^2 + \langle v_2^2 \rangle k_2^2 + \langle v_3^2 \rangle k_3^2 + 2\langle v_1 v_2 \rangle k_1 k_2$

A second type of model that embodies local convection may be suggested and compared. In general, four-component (but two-point) mixed velocity spectra may be defined, analogously to Eq. 5 by:

$$E_{ijkl}(x_2, x_2', \bar{k}, \omega) = \langle T_{ij}^*(x_2, \bar{k}, \omega) T_{kl}(x_2', \bar{k}', \omega') \rangle / \delta(\bar{k}' - \bar{k}) \delta(\omega' - \omega)$$

and two-component spectra by:

$$E_{ij}(x_2, x_2', \bar{k}, \omega) = \langle \hat{v}_i^*(x_2, \bar{k}, \omega) \hat{v}_j(x_2', \bar{k}', \omega') \rangle / \delta(\bar{k}' - \bar{k}) \delta(\omega' - \omega),$$

where \hat{v}_i is the transform of $v_i(\bar{x}, t)$ (cf. Eq. 7). Related spectra, $\epsilon_{ijkl}(\xi, \bar{k}, \omega)$ and $\epsilon_{ij}(\xi, \bar{k}, \omega)$, may be defined in terms of these just as M is defined in terms of $\hat{\sigma}$ in Eq. 9. If the same profile function $A(x_2, x_2')$ is factored out for all ϵ_{ijkl} and M , M is just a linear combination of the ϵ_{ijkl} . The local-convection model described above is thus expressed by:

$$\epsilon_{ijkl}(\xi, \bar{k}, \omega) = \epsilon_{ijkl}(\xi, \bar{k}) \int d^3 \bar{v}_c P(\xi, \bar{v}_c) \delta(\omega - u_c k_1 - \bar{v}_c \cdot \bar{k}) \quad (23)$$

In the second type of model the four-component spectra ϵ_{ijkl} are instead assumed to be given in terms of products of the two-component spectra ϵ_{ij} by the relations that would apply if the joint probability distribution of turbulent velocity at two points separated in both space and time (at fixed ξ) were normal¹⁰⁻¹² namely:

$$\begin{aligned} \epsilon_{ijkl}(\xi, \bar{k}, \omega) = & \int d^3 \bar{k}' [\epsilon_{ik}(\xi, \bar{k}', \omega') \epsilon_{jl}(\xi, \bar{k} - \bar{k}', \omega - \omega') \\ & + \epsilon_{il}(\xi, \bar{k}', \omega') \epsilon_{jk}(\xi, \bar{k} - \bar{k}', \omega - \omega')]. \end{aligned} \quad (24)$$

(The profile function factored out in the definition of the ϵ_{ij} in terms of the E_{ij} as in Eq. 9 is considered to be the square root of that factored out in the definition of the ϵ_{ijkl} . In the more usual instance of homogeneous turbulence

the profile function may be considered to be unity, and the argument ξ is absent from the ϵ_{ijkl} and ϵ_{ij} .) To this assumption of a space-time quasinormal distribution is adjoined the assumption of the local-convection model for the frequency dependence, not of the four-component spectra as before, but of the two-component spectra, i.e., Eq. 23 rewritten with ϵ_{ij} replacing ϵ_{ijkl} . This model leads to the relation between wavevector/frequency spectra and pure wavevector spectra given by:

$$\begin{aligned} \epsilon_{ijkl}(\xi, \bar{k}, \omega) = & \int d^3 \bar{v}_c \int d^3 \bar{v}_c' P(\xi, \bar{v}_c) P(\xi, \bar{v}_c') \int d^3 \bar{k}' \\ & \times \delta[\omega - u_c k_1 - (u_c' - u_c) k_1' - \bar{v}_c \cdot \bar{k} - (\bar{v}_c' - \bar{v}_c) \cdot \bar{k}'] \\ & \times [\epsilon_{ik}(\xi, \bar{k}', \omega') \epsilon_{jl}(\xi, \bar{k} - \bar{k}', \omega - \omega') + \epsilon_{jk}(\xi, \bar{k}', \omega') \epsilon_{il}(\xi, \bar{k} - \bar{k}', \omega - \omega')] \end{aligned} \quad (25)$$

where $u_c \equiv u_c(\xi, \bar{k} - \bar{k}')$, $u_c' \equiv u_c(\xi, \bar{k}')$, in contrast to the previously assumed relation given in Eq. 23.

In the non-convective tail, expression 23 is appreciable only if the normal component of wavevector is capable of generating frequency ω when convected at a velocity with normal component of the order of the rms normal turbulence velocity, i.e., $|k_2| \geq \omega/v_*$. In contrast, expression 25 yields an appreciable contribution from certain domains of the wavevector integral independently of k_2 , namely from domains of \bar{k}' such that $(\bar{v}_c' - \bar{v}_c) \cdot \bar{k}' \sim \omega$ or $(u_c' - u_c) k_1' \sim \omega$. Since no kinematic basis is identified for this result, the assumption of space-time quasinormality, Eq. 24, is suggested to be untenable or at least unfounded. Accordingly, we retain the local-convection model of Eq. 23.

6. Source Wavevector Spectra

We have now to formulate an appropriate model for the pure wavevector spectrum $M(\xi, \bar{k})$, that is, the source spectrum at fixed time. The principal model considered conforms to the picture of boundary-layer wave structure given by Kronauer and Morrison^{13,14} (see Fig. 3). These waves of fluctuating

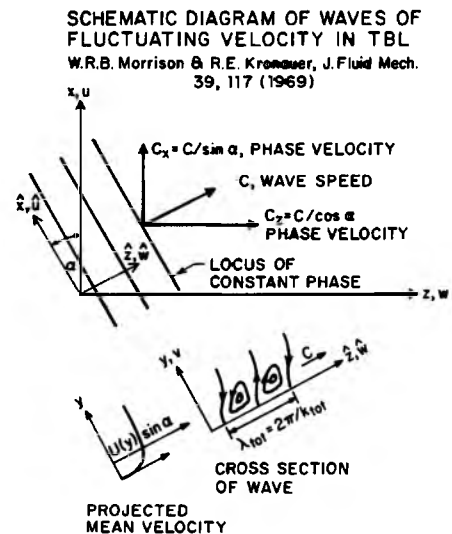


Fig. 3 Schematic Diagram of Waves of Fluctuating Velocity in TBL

velocity constitute a geometrically similar family for each direction of wave propagation in the wall-parallel plane and are coordinated over a range of wall distances. In a simple approximation for the layer of the log profile in a central range of wavenumbers, Morrison and Kronauer exhibit geometrically similar wave solutions of the linearized inviscid

Navier-Stokes equations that conform roughly to experimental wave properties. The phase velocity in the streamwise direction is found to match the mean velocity at a wall distance inverse to the planar wavenumber. For a wave having the direction of spatial independence, \hat{x} , at angle α to streamwise, the ratio of the fluctuating velocity component in this direction to those in the plane of the wave cross section is given by $\cot\alpha$.

These waves are invariant under a constant convection velocity and in this sense compatible with a local-convection model, provided that the normal component of convection velocity has the same dependence, if any, on wave direction α as do the fluctuating velocity components in the plane of the wave cross section.

Incorporating this wave structure into our model, then, we approximate the mean phase convection velocity, u_c , as independent of wall distance, or more particularly:

$$u_c = u(1/mK), \quad (26)$$

where the argument of the mean velocity $u(y)$ yielding u_c , i.e., the critical-layer depth, is supposed in Eq. 26 to scale on K^{-1} with coefficient $m^{-1} \approx 0.6^{13}$. Furthermore, we take the source wavevector spectrum to be the product of, first, a spectrum $M(\xi, K, k_2)$ independent of the direction of \bar{K} and formed only from the fluctuating velocity components in the wave cross section (normal to \hat{x}), second, a factor K^{-1} of geometric origin, and finally an anisotropy factor B_t :

$$M(\xi, \bar{k}) = v_*^4 B_t (\cos\theta) K^{-1} M(\xi, K, k_2), \quad \cos\theta = k_1/K \quad (27)$$

B_t is identified (within a constant factor) with the fourth-order two-direction spectrum of wave strength given in terms of the function $b_1(\alpha)$ defined in Ref. 13, appendix, by:

$$B_t(\cos\theta) = \langle [b_1^*(\pi/2-\theta)]^2 [b_1(\pi/2-\theta')]^2 \rangle / \delta(\theta'-\theta).$$

The cylindrical wave structures can retain spatial independence in the \hat{x} direction for only a finite distance, presumably scaled by boundary-layer thickness, and product form (27) therefore cannot be expected to hold for arbitrarily small K . At K less than this reciprocal length, it may crudely suffice to retain the product form but replace the factor K^{-1} by a factor such as $(K^2 + \alpha_0^2 \delta^{-2})^{-1/2}$ (α_0 constant), which is $\approx \delta$ for $K\delta \ll 1$.

Consideration of two-dimensional fluctuating flow in the wave cross section suggests assumption of the spectral form:

$$M(\xi, K, k_2) = \gamma_2 \gamma \xi^{-2\mu} (\gamma_2^2 k_2^2 + \gamma^2 K^2 + \xi^{-2})^{-1-\mu}, \quad (28)$$

in which the spatial correlation scales ($\gamma_2^{-1} \xi, \gamma^{-1} \xi$ with γ_1, γ_2 constant) are taken proportional to the geometric mean wall distance ξ . μ is an undetermined exponent not of critical importance but reasonably taken as zero so that the spectrum becomes scale-independent at high wavenumbers.

To indicate sensitivity to the assumed source wavevector spectrum, we consider also a form not based on the presumption of domination by Kronauer-Morrison waves but having the three wavevector components all entering in a parallel fashion:

$$M(\xi, \bar{k}) = v_*^4 C_t (\cos\theta) \gamma_1 \gamma_2 \gamma_3 \xi^{-2\mu} (\gamma_1^2 k_1^2 + \gamma_2^2 k_2^2 + \gamma_3^2 k_3^2 + \xi^{-2})^{-3/2-\mu} \quad (29)$$

The rough plausibility of forms (28) and (29) can be further supported by postulation of definite velocity spectra and assumption of a spatially quasinormal probability distribution.

7. Results for Wall Pressure

Using these alternative source spectra, we may perform in suitable approximations the final quadratures over geometric mean wall distance, ξ , and normal wavenumber, k_2 . We insert the source wavevector spectrum characteristic of Kronauer-Morrison waves, given by Eqs. 27 and 28, in Eq. 22 and substitute the result in Eq. 13 for P_t . In the non-convective tail defined by:

$$(\omega - u_c k_1) / v_* \gg (K^2 + \delta^{-2})^{1/2}, \quad (30)$$

we may, in the subject integral, neglect K and δ_1^{-1} relative to k_2 . Since then $\omega_k \approx \langle v_2^2 \rangle^{1/2}$ in Eq. 22, we require in Eq. 13 the dependence of $w(\xi) \langle v_2^2 \rangle^{-1/2}$ as well as of $\langle v_2^2 \rangle^{1/2}$ in the viscous and buffer layers. Near the wall, i.e., for $x_2, x_2' \ll 7\nu/v_*$, the four-component, two-point source intensity - and hence, by Eq. 11, $w(\xi)$ - presumably varies as $x_2^2 x_2'^2$, and the geometric mean of the rms normal component of fluctuating velocity at x_2 and x_2' varies as $(x_2^2 x_2'^2)^{1/2} [=x_2 x_2']$. This behavior is reflected and a plausible but convenient transition to the estimated outer values accomplished (with $w(\xi)$ normalized such that $w(\infty)=1$) by taking:

$$\langle v_2^2 \rangle^{1/2} / v_* = c_0 \xi^2 / (\xi^2 + \xi_0^2), \quad w(\xi) = \xi^4 / (\xi^2 + \xi_0^2)^2, \quad (31)$$

$$\xi_0 \equiv a_0 \nu / v_*, \quad \text{with } c_0 = 1, \quad a_0 = 5.$$

A dimensionless variable Ω defined by:

$$\Omega \equiv a_0 (\omega - u_c k_1) \nu / v_*^2 \ll 1 \quad (32)$$

characterizes the degree of suppression in the viscous sublayer. For $\Omega \ll 1$, this suppression is negligible (ξ_0 negligible in Eqs. 31), and we obtain a result for P_t given by:

$$P_t(\bar{k}, \omega) = a_t B_t (\cos\theta) \rho^2 v_*^7 K (\omega - u_c k_1)^{-4} \quad (33)$$

(in which a_t is a constant). For $\Omega \gg 1$, by evaluation of the pertinent double integral by steepest descents, we obtain a result for P_t given by Eq. 33 multiplied by a cutoff factor given roughly by:

$$0.2 \Omega^{5/3} \exp(-3.78 \Omega^{2/3}) \quad (34)$$

[According to the supposition following Eq. 27, unless $K\delta \gg 1$, the factor K in P_t of Eq. 33 should be replaced by $K^2 / (K^2 + \alpha_0^2 \delta^{-2})^{1/2}$.]

Using the alternative source spectrum (Eq. 29), we obtain results that differ from Eqs. 33 and 34 by a factor:

$$-K v_* / (\omega - u_c k_1). \quad (35)$$

Well down on the convective tail, we may omit the term $u_c k_1$ in Eq. 33. For the primary source spectrum the result (for $K\delta \gg 1$) then varies as v_*^7, ω^{-4} , and K . For the alternative spectrum, it varies as v_*, ω^{-5} , and K^2 , and is smaller than for the previous spectrum.

The main contributions in the quadratures that yield result (33) derive from wall distances $\xi \sim k_2^{-1}$, and, in the nonconvective tail, from normal wavenumbers $k_2 \sim (\omega - u_c k_1) / 2v_*$. As the viscous variable Ω increases, however, the erstwhile dominant

range of source distance is driven into the sublayer where contributions are suppressed, less on account of the decreasing turbulence intensity than by the decreasing local normal convection velocity. For $\Omega \gg 1$, the main contributions derive from distances near the edge of the sublayer, $\xi \sim \xi_0$, and from normal wavenumbers $k_2 \sim \Omega^{-1/3} (\omega - u_c k_1) / v_*$. This prediction of a strong viscous cutoff in the low-wavenumber pressure spectrum above relatively moderate values of Ω constitutes a characteristic consequence of the underlying model of fluctuating local convection when coupled with assumption of a probability distribution for fluctuating convection velocity, such as the normal distribution, that decreases rapidly at large velocities (see Appendix).

Thus far we have considered explicitly only the pure-turbulence contribution to pressure. We can proceed similarly to model also the mean-shear contribution. Explicitly, analogously to Eq. 13 we obtain:

$$P_m(\bar{k}, \omega) = 16\rho^2 v_*^2 \cos^2 \theta \int_0^\infty d\xi \xi \lambda(\xi) w_2(\xi) \int_{-\infty}^\infty dk_2 \varepsilon_2(\xi, \bar{k}, \omega) \times \sum_j c_{2j} K_o (2\xi [k_2^2 + (K + \delta_{2j}^{-1})^2])^{1/2}. \quad (36)$$

Here ε_2 is a spectrum of the normal component of velocity, $v_2(\bar{x}, t)$, in the same way that $M(\xi, \bar{k}, \omega)$ is a spectrum of a sum of velocity products, $v_1(\bar{x}, t) v_j(\bar{x}, t)$ (recall Eqs. 5-9), and $w_2(\xi)$, c_{2j} , and δ_{2j} are corresponding analogs of the earlier $w(\xi)$, c_j , and δ_j (recall Eq. 11). The factor $\lambda(\xi)$ in Eq. 36 is defined by representing the mean-velocity-derivative product approximately in the form:

$$u'(x_2) u'(x_2) = v_*^2 \lambda(\xi); \quad (37)$$

in the log-profile range, in particular, this form becomes correct with $\lambda(\xi) = (0.4\xi)^{-2}$. The local-convection model is expressed now by Eq. 20 with ε_2 replacing M . The model for $\varepsilon_2(\xi, \bar{k})$ referring to Kronauer-Morrison wave structure is expressed by Eq. 27 with ε_2 replacing M in both members, v_*^2 replacing v_*^4 , and $B_m(\cos\theta)$, say, replacing $B_t(\cos\theta)$. B_m is identified with the two-direction spectrum of wave strength given in terms of $b_1(\alpha)$ by¹³:

$$B_m(\cos\theta) = \langle (b_1^*(\pi/2 - \theta) b_1(\pi/2 - \theta')) \rangle / \delta(\theta' - \theta).$$

The specific functional form analogous to Eq. 28 is given by:

$$\varepsilon_2(\xi, k, k_2) = \gamma_2 \gamma K^2 \xi^{-2\mu} (\gamma_2^2 k_2^2 + \gamma_2^2 K^2 + \xi^{-2})^{-2-\mu}, \quad (38)$$

where, however, the coefficients γ_2 , γ , and μ may differ from those in Eq. 28. Similarly, a form analogous to the alternative spectrum (Eq. 29) is:

$$\varepsilon_2(\xi, \bar{k}) = v_*^2 c_m(\cos\theta) \gamma_1 \gamma_2 \gamma_3 K^2 \xi^{-2\mu} (\gamma_1^2 k_1^2 + \gamma_2^2 k_2^2 + \gamma_3^2 k_3^2 + \xi^{-2})^{-5/2-\mu}. \quad (39)$$

Apart from the angular dependence and a multiplicative constant, the structure, dependence, magnitude, and dominant domains of integration for the resulting pure-turbulence and mean-shear contributions are essentially similar. In the non-convective tail, however, we may question the meaningfulness of the mean-shear contribution when computed in this way. Specifically, since the pressure source for this contribution does not involve a convolution of fluctuating velocity transforms, we cannot contend on the same grounds as earlier for the pure-turbulence

source that the effective normal convection velocity at given wall distance should include all wavenumbers.

We can extend the previous results to include the domain of the convective peak as well as the non-convective tail. A convenient rough approximation that subsumes both domains is given for the nonviscous limit where $5K_t v / v_* \leq 1$ by:

$$P_t(\bar{k}, \omega) + P_m(\bar{k}, \omega) = [c_t B_t(\cos\theta) + c_m B_m(\cos\theta) \cos^2 \theta] \rho^2 v_*^3 K K_t^{-4} \quad (40)$$

$$\text{where } K_t^2 = (\omega - u_c k_1)^2 / (sv_*)^2 + K^2 + (b_1 \delta)^{-2} \quad (41)$$

The two terms in the bracketed factor giving angular dependence are associated respectively with pure-turbulence and mean-shear contributions. The mean-shear term contains an explicit $\cos^2 \theta$ factor as well as a factor $B_m(\cos\theta)$ related to the angular distribution of Kronauer-Morrison waves. Further consideration might indicate that B_t is just the square of B_m . In the domain of the convective ridge, the wavevector-frequency dependence of result (40) is characterized by a wavenumber K_t formed by adding in quadrature, first, the wavenumber K , second, a wavenumber measuring departure of k_1 from the value ω/u_c at the peak, and, third, a wavenumber $\propto \delta^{-1}$ characterizing the outer scale of the turbulent boundary layer. The coefficients s, b_1, c_t , and c_m are not strictly constant but vary only by factors of the order of two. Also, though not so indicated, s and b_1 may differ between the pure-turbulence and mean-shear contributions. Again, unless $K\delta \gg 1$, the factor K in Eq. 40 may be replaced by $K^2 / (K^2 + \alpha^2 \delta^{-2})^{1/2}$. In the instance of the alternative source spectrum, the factors $K K_t^{-4}$ in Eq. 40 (for all $K\delta$) are replaced by $K^2 K_t^{-5}$.

8. Comparison with Measured Properties Dominated by the Convective Domain

Calculation of quantities dominated by the convective ridge permits some limited check on elements of the model and may suggest the presently undetermined dependence on wavevector angle. Some such quantities are exactly or nearly independent of the source time dependence (or frequency spectrum) in the mean convected frame and hence do not at all check the model of local convection but do relate to the possible validity of the assumed source wavevector spectrum. These quantities include the spatial correlation of wall pressure at fixed time and the narrow-band cross-spectrum of point pressure for lateral separations (including as a special case the point pressure spectrum). The transform giving the spatial pressure correlation, $W_p(\zeta_1, \zeta_3, 0)$, for our specific source wavevector spectra, extended as required to $K\delta \ll 1$, reduces approximately to:

$$W_p(\zeta_1, \zeta_3, 0) = A_0 \rho^2 v_*^4 \int d^2 \bar{k} \exp(i\bar{k} \cdot \bar{\zeta}) K^2 (K^2 + \beta^2 \delta^{-2})^{-2} \times [c_t B_t(\cos\theta) + c_m B_m(\cos\theta) \cos^2 \theta], \quad (42)$$

where β represents a scale coefficient related to those defined earlier and A_0 a fixed numerical coefficient. A convenient ratio between the outer scale δ_1 for intensity in Eq. 13 and the scale $\alpha_0^{-1} \delta$ in the discussion following Eq. 27 referring to Kronauer-Morrison waves has been assumed, possible differences in scales for P_t and P_m ignored, and the integral over k_2 roughly approximated to yield Eq. 42. We now ask whether, consistent with measured results, the intrinsic anisotropy coefficients B_t

and B_m can be supposed independent of angle, corresponding to isotropic wave strength in the Kronauer-Morrison picture. If so, the measured anisotropy of pressure (at fixed time) is due only to the mean-shear contribution via the explicit factor $\cos^2\theta$. With $B_c=1$ and $B_m=1$, Eq. 42 yields:

$$W_p(\zeta_1, \zeta_3, 0) = \pi A_o (\rho v_*^2)^2 \{c_c [2K_o(z) - zK_1(z)] + c_m [K_o(z) - zK_1(z)] \cos^2\phi\} \quad (43)$$

where $z = \beta(\zeta_1^2 + \zeta_3^2)^{1/2} / \delta$, $\cos\phi = \zeta_1 / (\zeta_1^2 + \zeta_3^2)^{1/2}$. This result diverges at zero separation; hence a parameter must be introduced to characterize a high-wavenumber cutoff not explicitly provided in Eq. 40; in fits to available measurements the value of this parameter probably reflects mainly sensor size rather than the viscous length ν/v_* .

Fig. 4 shows contours of the normalized spatial correlation of wall pressure. Solid lines represent measurements by Bull¹⁵. Dotted lines represent the result obtained from Eq. 43 when two parameters are adjusted but only the $\cos^2\theta$ angular dependence is assumed, corresponding to the mean-shear contribution with isotropy of wave strength. Specifically, the dotted contours are obtained from the normalized correlation $W_p(\zeta_1, \zeta_3, 0) / \langle p^2 \rangle$, given by Eq. 43 with $c_c=0$, $\beta = \delta / 7.1\delta_*$, $\pi A_o c_m = \langle p^2 \rangle / 4.62(\rho v_*^2)^2$.

CONTOURS OF NORMALIZED SPATIAL CORRELATION OF WALL PRESSURE, $R_p(\zeta_1, \zeta_3, 0)$

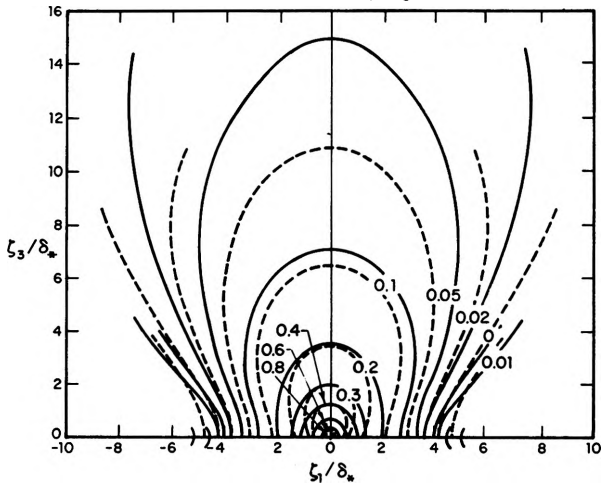


Fig. 4 Contours of Normalized Spatial Correlation of Wall Pressure

(According to present results, the type of plot in Fig. 4 is not universal, since δ/δ_* and $\langle p^2 \rangle / (\rho v_*^2)^2$ depend on Reynolds number.) Inclusion of an isotropic pure-turbulence contribution of comparable magnitude but somewhat smaller outer scale (that is, more rapid decrease of source intensity with wall distance) can improve agreement with experiment somewhat by making the contours approach isotropy more rapidly at small separations. If a $\cos^4\theta$ dependence is instead assumed, the contours are not drastically changed. Nevertheless, this comparison demonstrates at least the tenability within present considerations of the assumption that the intrinsic wave strength is isotropic. If this strength of velocity components in the cross section of the Kronauer-Morrison waves is isotropic, that of the component along the orthogonal direction of spatial independence varies in the linear theory as $\cot\alpha$, becoming large when this component is nearly streamwise.

Fig. 5 shows the normalized magnitude of cross-spectral density of pressure for lateral separation vs the usual similarity variable. Experimental points are those of Priestley as given in a paper by Corcos¹⁶, and curves representing the measurements by Bull and by Willmarth and Wooldridge²¹ are also shown. The theoretical curves are those obtained from our source wavevector spectrum (at large $\omega\delta/U_\infty$) for total angular dependence respectively as a constant, as $\cos^2\theta$, and as $\cos^4\theta$. If the intrinsic wave strength is isotropic, the pure-turbulence and mean-shear contributions yield a linear combination of the curves for a constant and for $\cos^2\theta$; such a result can evidently conform to that measured.

NORMALIZED MAGNITUDE OF PRESSURE CROSS-SPECTRUM FOR LATERAL SEPARATIONS

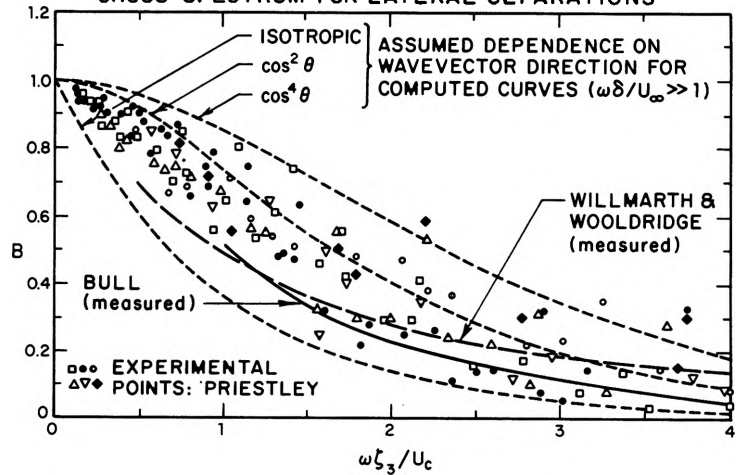


Fig. 5 Normalized Magnitude of Pressure Cross-Spectrum for Lateral Separations

As for the magnitude of the cross-spectral density for streamwise separation, the properties of the convective peak implied by our local-convection model for time dependence in the mean convected frame become pertinent. Partial computations indicate that results will conform well enough to measurement but probably not furnish substantial further information.

For skew separations, the magnitude of the predicted cross-spectral density will not have a product form for any of the assumed source spectra and angular dependences. Depending on the explicit form assumed, the magnitude tends to be roughly that obtained from the function giving the magnitude for purely streamwise or lateral separations by considering the two components to be added in quadrature. Curiously, measurements of pressure cross spectra seem never to have been made for separation directions chosen so as to test the functional form when both separation components are important, namely when the streamwise separation is about 7 times the lateral one¹⁷.

9. Comparison of Predicted Low-Wavenumber Pressure Spectra With a Wind-Tunnel Measurement

Returning to the low-wavenumber tail, we consider a recent wind-tunnel measurement by Jameson¹⁸ at BBN using a four-microphone array and improving an earlier experiment by Blake¹⁹. This yields an upper limit on the subject low-wavenumber pressure spectrum and perhaps actually measures it. Fig. 6 shows the nondimensionalized fractional-octave spectra vs Strouhal number measured at various flow speeds by the array

NONDIMENSIONAL FRACTIONAL OCTAVE SPECTRA MEASURED AT VARIOUS SPEEDS BY ALTERNATING PHASE MICROPHONE ARRAY (P.W. JAMESON, BBN Rept. 1937, 1970) WITH RELATED THEORETICAL SPECTRA

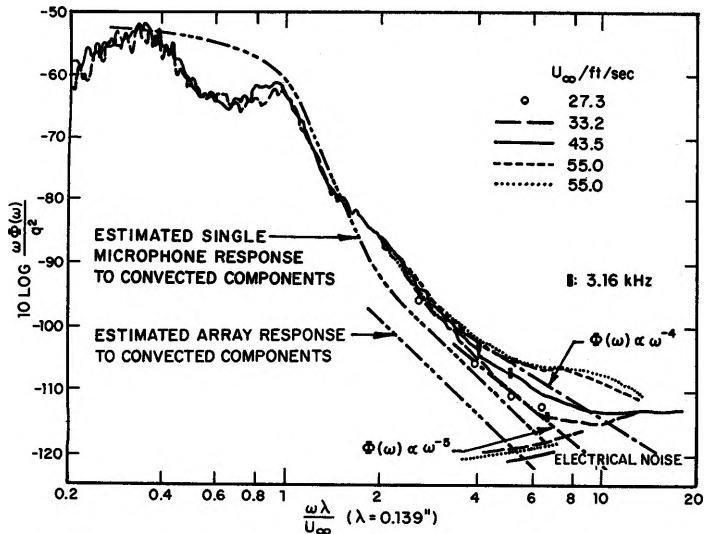


Fig. 6 Nondimensional Fractional Octave Spectra Measured at Various Speeds by Alternating Phase Microphone Array with Related Theoretical Spectra

with alternating phase. In a pertinent high-frequency range the measured spectra exceed the estimated convective contribution from the mean-convective ridge and in a certain range decrease with decreasing speed. This decrease may merely be due to decreasing relative acoustic contamination; possibly, on the other hand, it is due to the viscous suppression of the low-wavenumber TBL pressure spectrum predicted earlier, since the viscous frequency variable Ω becomes large enough at the lower speeds to activate this prediction. Under the assumption of viscous suppression, a line is drawn tangent to the high-speed results with the slope predicted for the inviscid domain from the local-convection model with Kronauer-Morrison source spectrum ($\phi \propto \omega^{-4}$). In the fitted form, namely:

$$P(\bar{k}, \omega) = a' \rho^2 v_*^7 K (\omega - u_c k_1)^{-4}, \quad (44)$$

this tangent yields an upper limit given by*

$$a' \leq 5. \quad (45)$$

Under the contrary assumption that the high-speed data are acoustically contaminated, another line is drawn tangent to the lower-speed result, this time with the higher slope predicted for the inviscid domain from the alternative source spectrum, on assumption - contrary to expectation - that viscous suppression has not yet entered ($\phi \propto \omega^{-5}$). In this second fitted form, namely:

$$P(\bar{k}, \omega) = a \rho^2 v_*^8 K^2 (\omega - u_c k_1)^{-5}, \quad (46)$$

this tangent yields:

$$a \leq 200. \quad (47)$$

The upper limit (45) under hypothesis (44) is smaller than the theory suggests, but not in clear conflict. The upper limit (47) under hypothesis (46) is reasonable (if one can account for the absence of appreciable viscous suppression in this

*This value refers to $P(\bar{k}, \omega)$ so normalized that mean squared pressure is represented by $\int_{-\infty}^{\infty} d\omega \int_{-\infty}^{\infty} dk_1 \int_{-\infty}^{\infty} dk_2 P(\bar{k}, \omega)$.

instance). Contributing to inconclusiveness is the further fact that the convective contribution may have been larger than estimated on account of microphone spatial sensitivity distributions different from that assumed.

CONCLUSIONS

In conclusion, a descriptive model of turbulent-boundary-layer pressure has been formulated and applied that is intended to be valid in the important domain of non-convective but incompressible wavenumbers. The objective was to construct a model which, if crude and shallow, is potentially useful and not totally arbitrary, being partly grounded in kinematics, similarity, and semiempirical accounts of boundary-layer structure. Whatever the fate of the tentative specific results presented for the scaling, dependence, and magnitude of pressure at low wavenumbers, the model is intended also to illuminate the range of possible results and their relation to assumed source properties. Further development is needed to clarify and assess the basic formulation and to construct more carefully, under competitive assumptions, the source spectra and the probability distribution for local convection velocity. More definite experimental investigation of the subject low-wavenumber domain, guided by such analytical modeling, is evidently essential to substantial further progress. Current wind-tunnel measurements of resonant plate excitation, it is hoped, will help to meet this requirement.

APPENDIX

We explore somewhat further here the dependence of $P_t(\bar{k}, \omega)$ in the non-convective tail on the assumed source spectrum.

Suppose first that the local-convection relation Eq. 22 is retained but that the wavevector spectrum $M(\xi, \bar{k})$ is obtained from the alternative form Eq. 29 by replacing ξ by δ ; i.e., consider a possible source spectrum with spatial correlation scales characteristic of the large-scale eddies of the outer boundary layer. We obtain for P_t in the non-convective tail Eq. 30 and nonviscous domain $\Omega \ll 1$ a dependence like that given for the previous alternative source spectrum by Eq. 33 and Eq. 35 but with a further factor $[(\omega - u_c k_1) \delta / v_*]^{-2\mu}$ adjoined if $\mu \neq 0$ in Eq. 29.

Now abandon the local-convection model of Eq. 20 entirely and assume, for example, the space/time-isotropic (but spatially anisotropic) source spectrum:

$$M(\xi, \bar{k}, \omega) = v_*^3 D_t (\cos \theta) \gamma_1 \gamma_2 \gamma_3 \gamma_4 \xi^{-2\mu} \times [\gamma_1^2 k_1^2 + \gamma_2^2 k_2^2 + \gamma_3^2 k_3^2 + \gamma_4^2 (\omega - u_c k_1)^2 / v_*^2 + \xi^{-2}]^{-2-\mu} \quad (A1)$$

(γ_1 constant, -1) [cf. (29)]. If $\mu < 1/2$, we obtain in the non-convective tail Eq. 30 a dependence like that given by Eq. 33 and Eq. 35 but with a further factor $[(\omega - u_c k_1) / v_* (K + \delta^{-1})]^{1-2\mu}$ adjoined. In this instance the dominant domain of integration in Eq. 13 is given by $\xi \sim k_2^{-1}$, $0 < k_2 \leq K + \delta^{-1}$. If $\mu > 1/2$, we obtain dependence like that given by Eq. 33 and Eq. 35, and the dominant range of k_2 extends over $0 < k_2 \leq (\omega - u_c k_1) / v_*$. Viscous suppression alters these results somewhat if, for $\mu < 1/2$, $5(K + \delta^{-1}) v_* / v_* \geq 1$ or, for $\mu > 1/2$, $\Omega \geq 1$. In either instance, however, contributions from low k_2 and hence from great wall distance ξ are unsuppressed,

in contrast to the exponential attenuation where $k_2 \ll (\omega - u_c k_1) / v_*$ in the case (Eq. 22) of the local-convection model with normal distribution of convection velocity; therefore, even where $\Omega \gg 1$, the source model (A1) does not yield sharp attenuation such as displayed by the factor (34).

For $\mu = -1/2$, we note parenthetically, the result given by (A1) for P_t in the nonconvective tail, as described above, assumes the form:

$$P_t(\bar{k}, \omega) \approx D_t(\cos\theta) \rho^2 v_*^6 (\omega - u_c k_1)^{-3} [1 + (K\delta_1)^{-1}]^{-2}, \quad (A2)$$

which, if $D_t = \text{constant}$, becomes wavevector-white where $k_1 \ll \omega / u_c$ and $K \gg \delta_1^{-1}$.

No kinematic or other basis is proposed for the illustrative source form (A1), though it may be approximately consistent with the previously discarded expression Eq. 25 derived from an assumed space/time-quasinormal velocity distribution (Ref. 10, Sec. 4.2).

SYMBOLS

$A(x_2, x_2')$	hypothetical pure-turbulence source profile factored out in definition of $M(\xi, \bar{k}, \omega)$	$u(x_2)$	mean velocity profile
$B_t(\cos\theta) [B_m(\cos\theta)]$	pure turbulence [mean-shear] source anisotropy factors for different source models.	U_∞	free-stream velocity
$C_t(\cos\theta) [C_m(\cos\theta)]$		v_*	friction velocity
$D_t(\cos\theta)$		\bar{v}_c	fluctuating convection velocity
		v_i	turbulent velocity components
c	fluid sound velocity	\bar{w}	total convection velocity
$\cos\theta$	k_1/K	$w(\xi) [w_2(\xi)]$	factor in pure-turbulence [mean-shear] source profile describing variation near wall
$\cos\phi$	ζ_1/ζ	$W_p(\zeta_1, \zeta_3, \tau)$	space-time correlation of wall pressure
$c_j, \delta_j [c_{2j}, \delta_{2j}]$	coefficients (c_j, c_{2j}) and length scales (δ_j, δ_{2j}) in factor of pure-turbulence [mean-shear] source profile describing variation away from the wall	x_2, x_2'	wall distances
$E(k, \omega)$	wavevector/frequency spectrum corresponding to ψ	$\bar{x} = (x_1, x_3)$	position vector parallel to wall
$k = (k_1, k_2, k_3)$	wavevector	α_0^{-1}	coefficient of correlation scale in direction normal to Kronauer-Morrison wave cross section
$\bar{k} = (k_1, k_3)$	wavevector parallel to wall	$\gamma_1^{-1}, \beta^{-1}$	coefficients in correlation scales
K_t	basic wavenumber variable that characterizes spectral density of wall pressure (Eq. 4)	$\delta[\delta_*]$	boundary layer [displacement] thickness
L	linear extent of a turbulent boundary layer	$\epsilon_2(\xi, \bar{k}, \omega) [-\epsilon_{22}]$	mean-shear source spectral density
$M(\xi, \bar{k})$	$= \int d\omega M(\xi, k, \omega)$ (likewise for other spectra)	$\epsilon_{ij}(\xi, \bar{k}, \omega)$	two-component velocity cross-spectra for geometric mean wall distance ξ
$M(\xi, K, k_2) [\epsilon_2(\xi, K, k_2)]$	pure-turbulence [mean-shear] source spectrum in Kronauer-Morrison wave cross section if factorable from $M(\xi, k, \omega) [\epsilon_2(\xi, k, \omega)]$	$\epsilon_{ijkl}(\xi, \bar{k}, \omega)$	four-component velocity cross-spectra of which $M(\xi, \bar{k}, \omega)$ is a linear combination
$M(\xi, \bar{k}, \omega)$	pure-turbulence source spectral density in frequency and three-dimensional wavevector related to $\bar{\sigma}$ at geometric mean wall distance ξ	$\bar{\zeta} = (\zeta_1, \zeta_3)$	separation vector parallel to wall
$\langle p^2 \rangle$	mean squared TBL wall pressure	$\zeta_2 [=x_2' - x_2]$	normal separation
$P(\bar{k}, \omega)$	wavevector/frequency spectral density of wall pressure	θ_1	k_1/K
$P(\xi, \bar{k}, \bar{v}_c)$	probability density for fluctuating convection velocity \bar{v}_c referring to wavevector \bar{k} and geometric mean wall distance ξ	μ	parameter (exponent) in various model source wavevector spectra (Eqs. 28, 29, 38, 39, A1)
\bar{r}	separation vector	ν	kinematic viscosity
s, b_1, c_t, c_m	nearly constant coefficients in calculated spectral density wall pressure	$\xi [= (x_2, x_2')^{1/2}]$	geometric mean wall distance
$\hat{T}_{ij}(x_2, \bar{k}, \omega)$	wavevector/frequency transform of turbulent velocity product $v_i v_j$ at wall distance x_2	$\xi_0 [= a_0 \nu / v_*, a_0 \approx 5]$	viscous sublayer thickness
u_c	effective convection velocity (=pressure phase velocity)	ρ	fluid mass density
		$\bar{\sigma}(x_2, x_2', \bar{k}, \omega)$	pure-turbulence source spectrum/profile of pressure
		τ	time delay
		$\phi(\omega)$	frequency spectral density of wall pressure area-averaged by microphone or array
		$\psi(\bar{r}, \tau)$	space/time correlation for statement of local-convection approximation
		$\Omega [= a_0 (\omega - u_c k_1) \nu / v_*^2]$	dimensionless viscous cutoff frequency
		ω	radian frequency

REFERENCES

- Bergeron, R. F., Jr., "The Low Wavenumber Component of Wall Pressure in a Nearly Incompressible Turbulent Boundary Layer," Bolt Beranek and Newman Inc., Rept. 1750, Nov. 1968.
- Van Dyke, W., Perturbation Methods in Fluid Mechanics, Academic Press, New York, 1964.
- Ffowcs Williams, J. E., J. Fluid Mech., **22**, 507 (1965).
- Landahl, M. T., J. Fluid Mech., **29**, 441 (1967); "A Wave-Guide Model for Turbulent Shear Flow," NASA CR-317, Oct. 1965.
- Kraichnan, R. H., J. Acoust. Soc. Am., **28**, 378 (1956).
- Chase, D. M., "The Low-Wavenumber Spectral Density of Turbulent-Boundary-Layer Pressure and Its Role in Plate Vibration and Radiation," P. 169, Proc. 2nd U.S./Fed. Rep. Germany Hydroacoustics Symposium, Orlando, Fla., Jan. 1971.
- Laufer, J., "Investigation of Turbulent Flow in a Two-Dimensional Channel," NACA Rept. 1053, 1951.
- Lumley, J. L., Phys. Fluids, **8**, 1056 (1965).
- Favre, A. J., Trans. ASME, J. Appl. Mech., **E32**, 241 (1965).
- Chase, D. M., Acustica, **22**, 303 (1969/70).
- Batchelor, G. K., The Theory of Homogeneous Turbulence, Cambridge University Press, 1953.

12. Chandrasekhar, S., Proc. Roy. Soc., 229A, 1 (1955).
13. Morrison, W. R. B., and Kronauer, R. E., J. Fluid Mech., 39, 117 (1969).
14. Morrison, W., Bullock, K., and Kronauer, R., J. Fluid Mech., 47, 639 (1971).
15. Bull, M. K., J. Fluid Mech., 28, 719 (1967).
16. Corcos, G. M., J. Sound Vibration, 6, 59 (1967).
17. Chase, D. M., J. Acoust. Soc. Am., 46, 1350 (1969).
18. Jameson, P. W., "Measurement of Low Wavenumber Component of Turbulent Boundary Layer Wall Pressure Spectrum," Bolt Beranek and Newman Inc., Rept. 1937, Sept. 1970.
19. Blake, W. K., and Chase, D. M., J. Acoust. Soc. Am., 49, 862 (1971).
20. Priestley, J. T., "Correlation Studies of Pressure Fluctuations on the Ground Beneath a Turbulent Boundary Layer," NBS Rept. 8942, July 1965.
21. Willmarth, W. W., and Wooldridge, C. E., J. Fluid Mech., 14, 187 (1962).

DISCUSSION

W. K. BLAKE (Naval Ship Research and Development Center): In the low-wavenumber tail was it the mean-shear or turbulence-type interaction that dominated?

CHASE: When I formally made the same assumption concerning the probability of local convection velocity for the mean-shear contribution that I made for the pure-turbulence term, they

proved to be comparable, though the mean-shear part, by some appropriate measure, is suggested to be larger by a modest factor. The justification I offered for using that probability distribution, however, really fails for the mean-shear contribution. I rather suspect that the justification I offered is not the true one, but that in fact the assumption I made is roughly correct. In any case, if you credit my assumption that the probability distribution of the local convection velocity in both instances conform roughly to the probability of the local total turbulence velocity, the two contributions are of the same order. It is just that one might question this assumption in the case of the mean-shear contribution in the low-wavenumber tail. In the convective region, on the other hand, this difference did not arise, and there, with one fewer element of uncertainty, the two contributions were concluded to be comparable.

S. J. KLINE (Stanford University): Dick Lahey's results (Ref. 16 of our paper) correlate not only velocity perturbations but perturbations in pressure, density and adiabatic temperature. It is a different kind of a model, and you might want to look at that. It does for example fit Corcos' accepted correlation for pressure fluctuations very well. In fact, Corcos' form simply drops out of the more general equation. Lahey's original form does include your ω , if I read your symbols correctly, and Lahey also integrates in a similar way.